Journal of Environmental Chemical Engineering 10 (2022) 108415

Contents lists available at ScienceDirect

Journal of Environmental Chemical Engineering

journal homepage: www.elsevier.com/locate/jece

Effects of desloratadine on activated sludge: Behaviour of EPS and sludge properties

Antonio Melo [a,b], Joana Costa [a,b], Cristina Quintelas [a,b], Eugénio C. Ferreira [a,b], Daniela P. Mesquita [a,b,*]

[a] CEB - Centre of Biological Engineering, University of Minho, 4710-057 Braga, Portugal
[b] LABBELS - Associate Laboratory, Braga, Guimarães, Portugal.

ARTICLE INFO

Editor: Dr. Y. Liu

Keywords:
Activated sludge
Desloratadine
Loosely bound EPS
Tightly bound EPS
Quantitative image analysis
Three-dimensional excitation emission-matrix

ABSTRACT

Desloratadine (DESL), a second generation of antihistamines, is an important anti-allergic pharmaceutical used to treat allergic rhinitis, hay fever and urticaria. In this study, the overall performance, extracellular polymeric substances (EPS) production, and sludge properties were assessed in a sequencing batch reactor wastewater treatment process with activated sludge during 139 days, under the presence of DESL (1, 5, and 10 mg L^{-1}). DESL at 10 mg L^{-1} impacted biomass activity decreasing the chemical oxygen demand removal (78%) and the ammonium removal (71%). The removal of DESL was of 63%. Tightly bound EPS (TB-EPS) was significantly higher (149.5 mg g_{MLVSS}^{-1}) at the end of operation. Peaks attributed to protein-like fluorophores clearly predominated along the experimental phases using three-dimensional excitation-emission matrix (3D-EEM) fluorescence. The peak locations and intensities in the EPS fluorescence revealed the difference in the chemical structures of the EPS caused by DESL exposure. Quantitative image analysis results clearly demonstrated the formation of large aggregates. Principal component analysis (PCA) showed a positive relationship between TB-EPS components, and large aggregates. Moreover, the results allowed to distinguish the different operational phases, emphasizing the effect of DESL on EPS and aggregates.

1. Introduction

Pharmaceutical compounds are of great concern because of their potential toxicity. These compounds are gaining increasing attention due to their fate in the aquatic environment and partial removal in wastewater treatment plants (WWTP) [1–3]. Pharmaceutical compounds are introduced into the environment mainly as a result of human excretion, untreated sewage, decentralized systems and centralized WWTP, and inappropriate disposal of unused drugs [4]. Due to their widespread use and diverse applications, antihistamines have become the largest class of pharmaceuticals employed to treat allergic diseases, with more than 45 antihistamines currently on the market [5]. These compounds have been commonly detected in influent wastewater [6], effluent discharges from WWTP [7], and surface waters [8]. About 15 antihistamines, including desloratadine (DESL), have been detected in watercourses in concentrations ranging from ng L^{-1} to μg L^{-1} [4]. Pharmaceuticals are also being detected in higher ranges (mg L^{-1}), for example in the case of cetirizine (antihistamine) and ciprofloxacin (antibiotic) [7,10]. DESL, a second-generation antihistamine is widely prescribed to treat allergic reactions and causes less drowsiness compared to other pharmaceuticals and their toxic effects were previously reported to affect organisms selected from two trophic levels [11]. The results revealed similar toxicity of DESL among the organisms tested and most chronically effective in two of the four organisms evaluated [11].

Excreted by microorganisms, extracellular polymeric substances (EPS), mainly composed by proteins (PN), polysaccharide (PS), and humic acid substances (HAS), are involved in microbial aggregates structure through complex interactions due to their physicochemical properties [12–15]. It is known that under toxic conditions, microorganisms in activated sludge (AS) can vary the EPS concentration, hence influencing the performance of the biological process [16]. Thus, it is suggested that EPS can make a certain contribution to pharmaceutical compounds removal from aqueous environments and in the sludge biosorption process, due to abundant functional groups and binding sites [17]. However, so far, little information has been available in terms of

* Corresponding author at: CEB - Centre of Biological Engineering, University of Minho, 4710-057 Braga, Portugal.
E-mail address: daniela@deb.uminho.pt (D.P. Mesquita).

https://doi.org/10.1016/j.jece.2022.108415
Received 2 May 2022; Received in revised form 22 July 2022; Accepted 8 August 2022
Available online 8 August 2022

EPS in AS biomass under DESL exposure.

Quantitative Image Analysis (QIA) has proven to be a suitable tool for monitoring biological treatment systems [18], as well as the structural assessment of biological aggregates in AS, including the identification of AS dysfunctions, namely filamentous bulking and non-filamentous bulking [19]. Furthermore, methodologies of multivariate statistics, such as PCA, have become increasingly important in improving biological processes analysis, mainly in organizing and extracting relevant information from such comprehensive datasets [20].

3D-EEM fluorescence spectroscopy is a rapid, selective and sensitive technique, offering useful information regarding the fluorescence characteristics of compounds such as protein-like fluorophores and humic-like fluorophores in EPS [21]. Furthermore, the composition of EPS has been widely characterized by 3D-EEM spectroscopy since fluorescence characteristics can be applied to elucidate the functional groups and element composition in EPS samples [22].

Although the presence and removal of pharmaceutical compounds in wastewater treatment (WWT) systems has been intensively investigated in the last two decades, there is scarce information in the literature on the impact and removal of DESL in biological WWT, namely AS systems.

Considering the above, the purpose of this study was to provide deep insights regarding the impact of DESL on AS systems performance, including the production and composition of EPS. DESL was used in a range of concentrations present in pharmaceutical industry and in hospital wastewaters. QIA and multivariate statistical analysis were applied to improve the biological process evaluation.

2. Materials and methods

2.1. Experimental procedure

In this work, a sequencing batch reactor (SBR) with a working volume of 2 L was inoculated with AS from a full-scale WWTP and fed with synthetic wastewater (the composition can be found in [23]). The initial mixed liquor suspended solids (MLSS) in the system was ca. 3 g L^{-1}. The reactor was operated at room temperature with 6 h cycles, including 40 min of feeding, 240 min of aeration, 40 min of settling, and 40 min of withdrawal. For aeration, fine air bubbles were supplied through a porous stone at the bottom of the reactor. The sludge retention time was set at approximately 10 days by controlling the amount of suspended sludge discharged daily, and the hydraulic retention time was 12 h with a volumetric exchange ratio of 50%. The experimental setup can be found as supplementary information – SI (Fig. S1). During phases II-IV, DESL was added to the synthetic wastewater in order to reach a concentration in the inlet feeding, as indicated in Table 1.

Quantification of chemical oxygen demand (COD), ammonium (NH_4^+-N), nitrite (NO_2^--N), and nitrate (NO_3^--N) was performed as described by Melo et al. [23]. MLSS, mixed liquor volatile suspended solids (MLVSS), and the sludge volume index at 30 min (SVI) were determined in accordance with standard methods [24]. DESL quantification was assayed as previously described by Quintelas et al. [25]. Briefly, DESL quantification was performed for the inlet feeding and effluent, with all collected samples filtered with a 0.2 μm filter prior to HPLC analysis. The analysis was performed using a Nexera UHPLC equipment (Shimadzu Corporation, Tokyo, Japan) with a Kinetex 5 u EVO C18 column (150 × 4.6 mm i.d.) supplied by Phenomenex, Inc. (CA, USA). The mobile phase was potassium dihydrogen phosphate (0.05 M; pH 3) (pump A), acetonitrile (pump B) and methanol (pump C). An isocratic method was employed with 45% A, 48% B and 7% C. The flow rate was 0.8 mL min^{-1}. The samples were monitored by a diode array detector from 190 to 400 nm, and chromatograms were extracted at 247 nm. The column oven was set at 25 °C, and the injection volume was 12 μL.

Table 1
DESL concentrations at the inlet feeding throughout SBR operation.

Phase	Operation days	DESL inlet concentration (mg L^{-1})
I	0–34	0
II	35–69	1
III	70–105	5
IV	106–139	10

2.2. EPS extraction and quantification

The EPS extraction was based on the method developed by Li and Yang [26] and previously modified by Melo et al. [23] and both the LB-EPS and TB-EPS extractions were analysed for PS, PN, and HAS using colorimetric methods [23].

Extracted EPS samples were also evaluated by 3D-EEM spectra, using a luminescence spectrophotometer (Aqualog, Horiba). The 3D-EEM spectra were collected with subsequent scanning emission spectra from 240 to 600 nm at 5 nm increments by varying the excitation wavelength from 240 to 600 nm at 5 nm sampling intervals. The excitation and emission splits were maintained at 5 nm and 2.5 nm, respectively. The 3D-EEM data were processed using the software Origin 8.0.

The EEM spectrum can be divided into regions based on the specific excitation and emission wavelength pair. The organic substances present in the EPS, such as protein-like and humic acid-like substances, could be depicted by the percent fluorescence response ($P_{i,n}$), according to Chen et al. [27], Yang et al. [28], and Qian et al. [29]. In the present study excitation and emission boundaries were defined into two regions associated with peaks containing excitation wavelengths of 250- ≈ 280 nm and emission wavelengths < 380 nm for protein-like substances (region A). Peaks with excitation wavelengths > 280 nm and longer emission wavelengths (>380 nm) are related to humic acid-like substances (region B).

2.3. Sludge sampling, QIA, PCA and statistical analysis

The sampling procedure and QIA analysis were achieved as previously described [23]. PCA was performed using the SBR physicochemical parameters, EPS concentration and composition, and the main QIA parameters. A total 60 observations and 19 variables were used to compose the dataset matrix. The goal of the employed PCA was to find interrelationships between the parameters that compose the dataset matrix. The PCA was performed with Matlab 8.5 software (The MathWorks, Inc. Natick, USA). The analysis of variance (ANOVA) using Tukey's post-hoc test was applied to evaluate significant difference in the removal of COD, NH_4^+-N and DESL between all operational phases and assess variations in EPS concentration and its components. Statistical analysis was performed using the SPSS program (IBM, Armonk, NY, Version 26.0).

3. Results and discussion

3.1. SBR behaviour

The concentrations of COD, ammonium (NH_4^+-N), nitrite (NO_2^--N), and nitrate (NO_3^--N) during the SBR operation are shown in Fig. 1a,b. In the absence of DESL (phase I), the COD at the outlet was < 25 mg L^{-1} (Fig. 1a), with a COD removal efficiency of 96% (on average) (SI - Table S1). During phase II and phase III, the COD removal efficiency slightly decreased, on average, to 88% and 87%, respectively (SI - Table S1). During phase IV (feeding with 10 mg L^{-1} of DESL), the average COD removal efficiency decreased significantly ($p < 0.05$) to 78% (SI - Table S1-S3). The concentration of NH_4^+-N in the effluent was very low during phases I-III (Fig. 1b), indicating high removal efficiencies around 94–100% (SI - Table S1). Higher NH_4^+-N effluent concentrations were found in phase IV, in the presence of 10 mg L^{-1} of DESL, decreasing significantly ($p < 0.05$) the NH_4^+-N removal efficiency

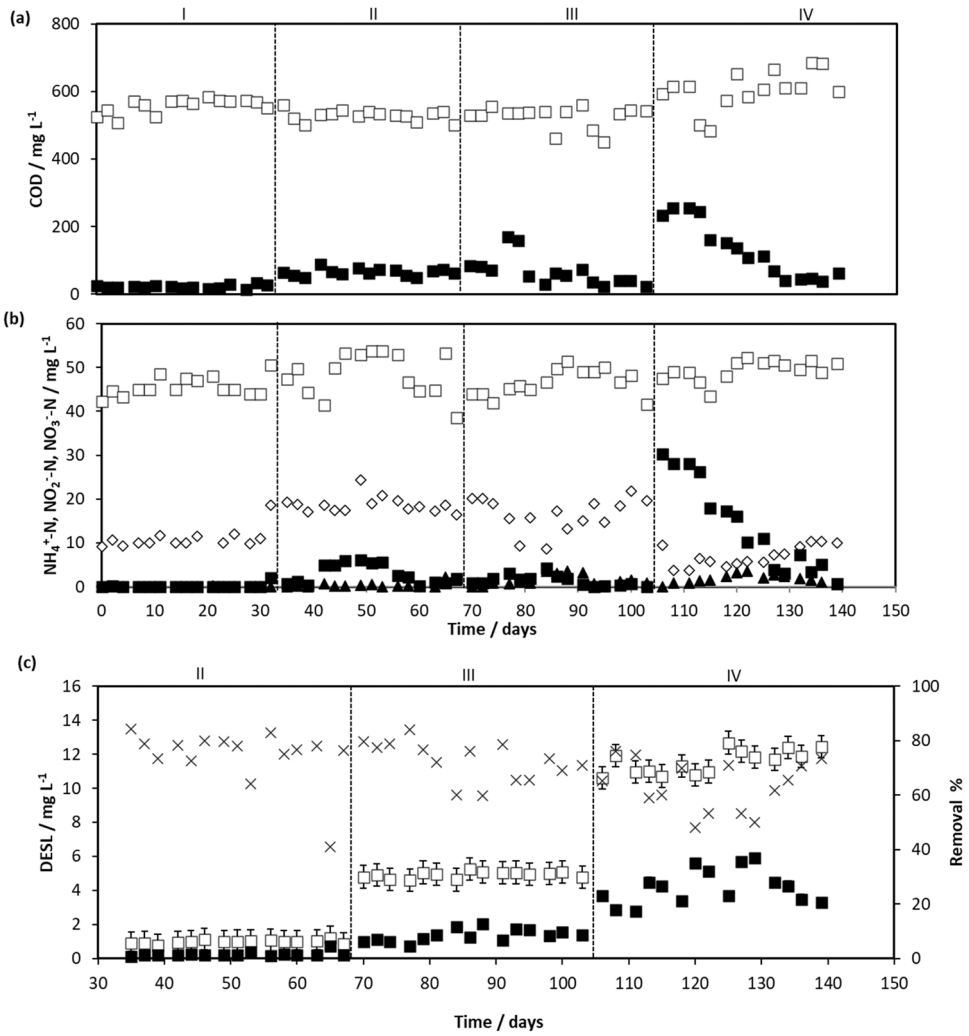

Fig. 1. SBR performance profile in terms of COD, NH_4^+-N, NO_2^--N, NO_3^--N, and DESL concentration. (a) COD in the inlet feeding (□), and in the effluent (■); (b) NH_4^+-N in the inlet feeding (□), in the effluent (■), NO_2^--N in the effluent (▲), and NO_3^--N in the effluent (◇); (c) DESL in the inlet feeding (□), in the effluent (■), and removal efficiency (×). Operational phases I-IV.

to 71% (on average) (SI - Table S1-S3). Throughout phases I-II, NO_2^--N concentrations in the effluent were at residual levels, and increased during phases III-IV (Fig. 1b, SI - Table S1). Concerning the NO_3^--N profile in the effluent, an increasing trend occurred along phases I-III and reduced during phase IV (Fig. 1b, SI - Table S1). The present results seem to demonstrate that DESL impacted biomass activity, which are in agreement with previous works that assessed the effect of pharmaceutical compounds in biological systems, mainly in the organic matter removal [30], and in nitrification process [31,32].

Fig. 1c shows the profile of DESL concentration and removal efficiency along SBR operation. On average, DESL effluent concentrations were 0.3 mg L^{-1} (phase II), 1.4 mg L^{-1} (phase III) and 4.2 mg L^{-1} (phase IV). Therefore, average removal efficiencies of 75%, 73% and 63% were obtained for DESL during phase II, III and IV, respectively (SI - Table S1). In addition, DESL removal efficiencies in phase IV were significantly different ($p < 0.05$) from phases II-III (SI - Tables S2 and S3).

DESL has proven to be toxic for organisms of the aquatic trophic chain [11]. It was investigated the acute and chronic ecotoxicity of DESL in green alga *Pseudokirchneriella subcapitata*, in planktonic rotifer *Brachionus calyciflorus* abundant in freshwaters, in anostracan crustacean *Thamnocephalus platyurus*, highly sensitive in acute toxicity testing and in cladoceran crustacean *Ceriodaphnia dubia*, often employed in acute and chronic toxicity testing. The results revealed the occurrence of toxic effect in both acute and chronic assays. Regarding acute toxicity testing, DESL was able to cause 50% of mortality in *B. calyciflorus* at 1.2 mg L^{-1} and *C. dubia* at 1.5 mg L^{-1}, differently from the effects found in *T. platyurus* that was necessary a much higher concentration (6.2 mg L^{-1}). On the other hand, chronic toxicity results revealed that DESL was chronically active compound both in *C. dubia*, with a median effective concentration of 9.4 μg L^{-1}, and in the green alga *P. subcapitata* (EC50 = 220.2 μg L^{-1}). Therefore, as AS is composed by a mixed microbial culture, 10 mg L^{-1} of DESL could affect some specific microorganisms, which might explain the decrease in the DESL removal efficiency during phase IV. This result corroborates studies where the removal of other antihistamines and psychiatric drugs decreased over time [33–38]. The loss of pharmaceutical compounds removal could be attributed to a bacterial shift in the biological process.

3.2. EPS production, composition, and assessment by 3D-EEM

Fig. 2a shows LB-EPS and TB-EPS content. LB-EPS content of 49.5 mg g_{MLVSS}^{-1} was achieved during phase I, whereas 100.0, 96.2, and 74.9 mg g_{MLVSS}^{-1} were obtained, on average, for phase II, III and IV, respectively (Fig. 2a, SI - Table S4). Accordingly, LB-EPS content showed significant differences ($p < 0.05$) between phase I and phases II-III (SI - Tables S5, S6). During phase IV, LB-EPS decreased, suggesting that 10 mg L^{-1} of DESL can influence the contents of LB-EPS by affecting the

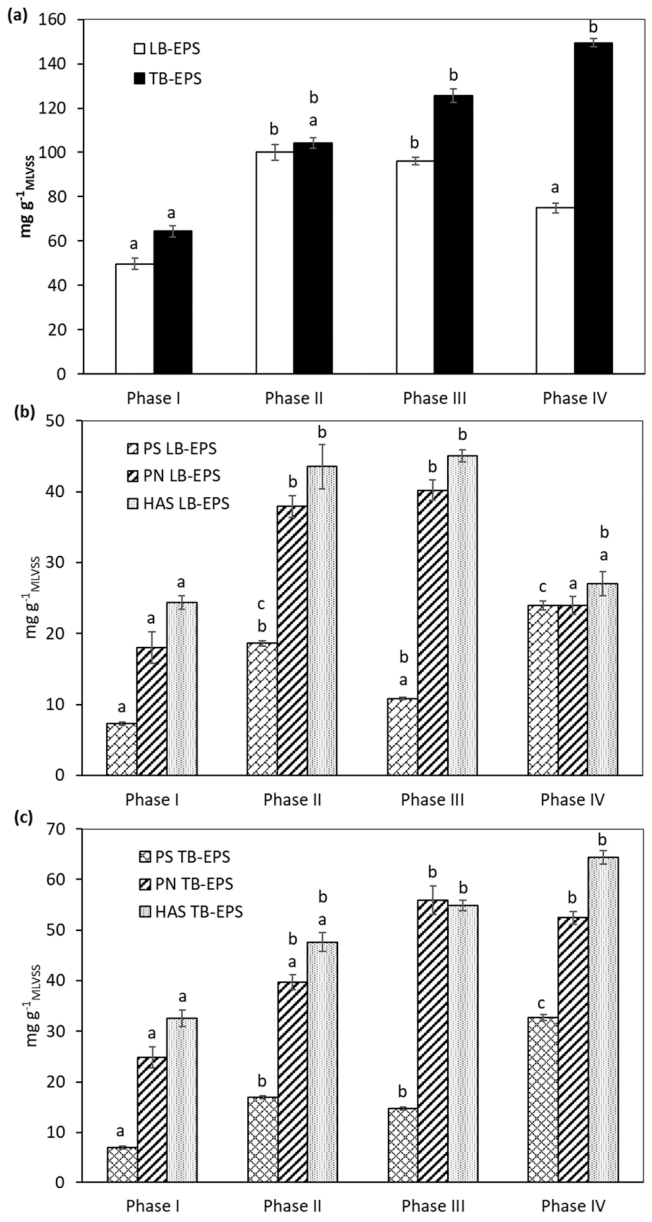

Fig. 2. LB-EPS and TB-EPS in terms of PS, PN, and HAS components. (a) LB-EPS and TB-EPS content for different phases of SBR operation; (b) PS, PN, and HAS content of the LB-EPS; (c) PS, PN, and HAS content of the TB-EPS. Bars with different letters present statistically significant differences ($p < 0.05$).

metabolism of the microorganisms. Li et al. [37] reported similar results of LB-EPS in SBR when copper Cu(II) was added during a long-term period. LB-EPS increased after adding Cu(II) and then decreased slightly. For these authors, the increase in LB-EPS content indicated a microbial response to relieve the sudden exposure to Cu(II). Indeed, LB-EPS is regarded as the primary surface for contact and interaction with toxic compounds [39]. Also, according to Miao et al. [22] the increase in toxicity caused by copper oxide (CuO) nanoparticles stimulated the production of EPS, especially LB-EPS, due to their presence in the upper layers of biofilm, and may have functioned as the primary surface for contact and interaction with CuO [22]. In this way, the decrease of LB-EPS can be attributed to the rise of larger aggregates, leading to the increase of TB-EPS content during phase IV.

From phase I to phase IV, an increase in the TB-EPS content was obtained, reaching 149.5 mg g^{-1}_{MLVSS} in phase IV (Fig. 2a, SI -Table S4). Significant differences ($p < 0.05$) were found between phase I and phases III-IV (SI - Tables S5, S6). The increase in TB-EPS production can be considered a defence mechanism for microorganisms in the presence of toxic substances [38,40–42]. As along phases II-IV an increase in TB-EPS content occurred, it can be concluded that DESL directly interferes with AS metabolic activity. Consequently, the increase in TB-EPS content during SBR operation may have contributed to a high relative abundance of large aggregates [23,43,44].

The LB-EPS components from phase I to phase IV are shown in Fig. 2b. For PS the results obtained during phases I and III were similar, and the content increased significantly ($p < 0.05$) in phase II and IV (SI – Tables S5, S6). PN in the presence of DESL (phases II-III) increased to the highest levels, statistically different ($p < 0.05$) from phase I (Fig. 2b, SI - Tables S5, S6). During phase IV, PN decreased to levels close to phase I. In this way, PN showed significant differences ($p < 0.05$) between phases I-IV and phases II-III. For HAS, a significant difference ($p < 0.05$) was solely observed between phase I and phases II-III (Fig. 2b, SI Tables S5, S6). The TB-EPS components from phase I to phase IV are shown in Fig. 2c. For PS, a significant difference ($p < 0.05$) was found between phase I and phases II-IV (SI - Tables S5, S6). For PN, a significant change was obtained between phase I and phases III-IV. HAS content increased from phase I to phase IV.

The addition of DESL has led to a variation in the PS and PN proportions for each experimental phase. Several studies have demonstrated that changes in the operational parameters (pH, temperature, toxic compounds, etc.) might affect the yield and composition of different fractions of EPS produced by microorganisms [45,46]. In our research, LB- and TB-EPS contained a large portion of proteins (PN/PS ratio = 1.0 – 2.5, and 1.6 – 3.6, respectively). Interestingly, from the middle to the end of phase III, PN/PS ratio presented the highest values (3.7 and 3.8) for LB- and TB-EPS, respectively, which likely influenced the rise of large aggregates. This result corroborates the previous study of Xu et al. [47], where the increase of the PN/PS ratio was considered crucial in the formation of large aggregates (during the granulation process) due to hydrophobic (PN) and hydrophilic (PS) characteristics of EPS components [48]. It has been also reported that a sharp increase in PN was recognized to be crucial for the long-term stability of AS [49]. The results found in the present research revealed that pharmaceutical compounds (especially antihistamines), favoured the increase in EPS production for bacterial self-defence, especially TB-EPS.

Figs. 3 and 4 present 3D-EEM results of sludge EPS at the beginning, middle and end for each phase, and peaks fluorescence intensity are displayed in Table 2. Samples were analysed by 3D-EEM fluorescence spectroscopy to characterize changes in the organic compounds present in the EPS which have fluorescent characteristics, such as protein-like, humic acid-like and fulvic acid-like substances [50,51]. The 3D-EEM fluorescence spectra of LB-EPS and TB-EPS under DESL exposure revealed relationships between the characteristic peaks' intensities and the EPS components. The shifts of the fluorescence peaks can provide information on the chemical structural changes of the EPS, being related to the change of some enzyme activities, the biosynthetic and metabolic pathways of the organics and the redistribution of the metabolic flux with the increase of DESL concentration [52].

Four peaks could be detected from the 3D-EEM fluorescence results. Peak A and peak B representing protein-like substances (peak A, Ex/Em = 270–275/300–305; peak B, Ex/Em = 270–275/370–375), peak C for fulvic acid-like substances (peak C, Ex/Em = 297–303/420–445), and finally peak D representing humic acid-like substances (peak D, Ex/Em = 320–360/414–451).

In the beginning of phase I (day 0), LB-EPS was composed mainly of proteins-like substances (peak B) (Fig. 3a). After that, LB-EPS composition slightly increased humic (peak D) and fulvic acid-like substances (peak C) on day 32. During phase II, the fluorescence intensity of the peaks C and D from day 35 till day 67 increased (Fig. 3b). Additionally, the fluorescence intensity of peak B, representing the protein-like substances, had similar behaviour during phases I and II. During phases III and IV (Fig. 3c-d), peaks C and D showed a decreasing trend from day 70 onwards and protein-like substances prevailed (peaks A and B).

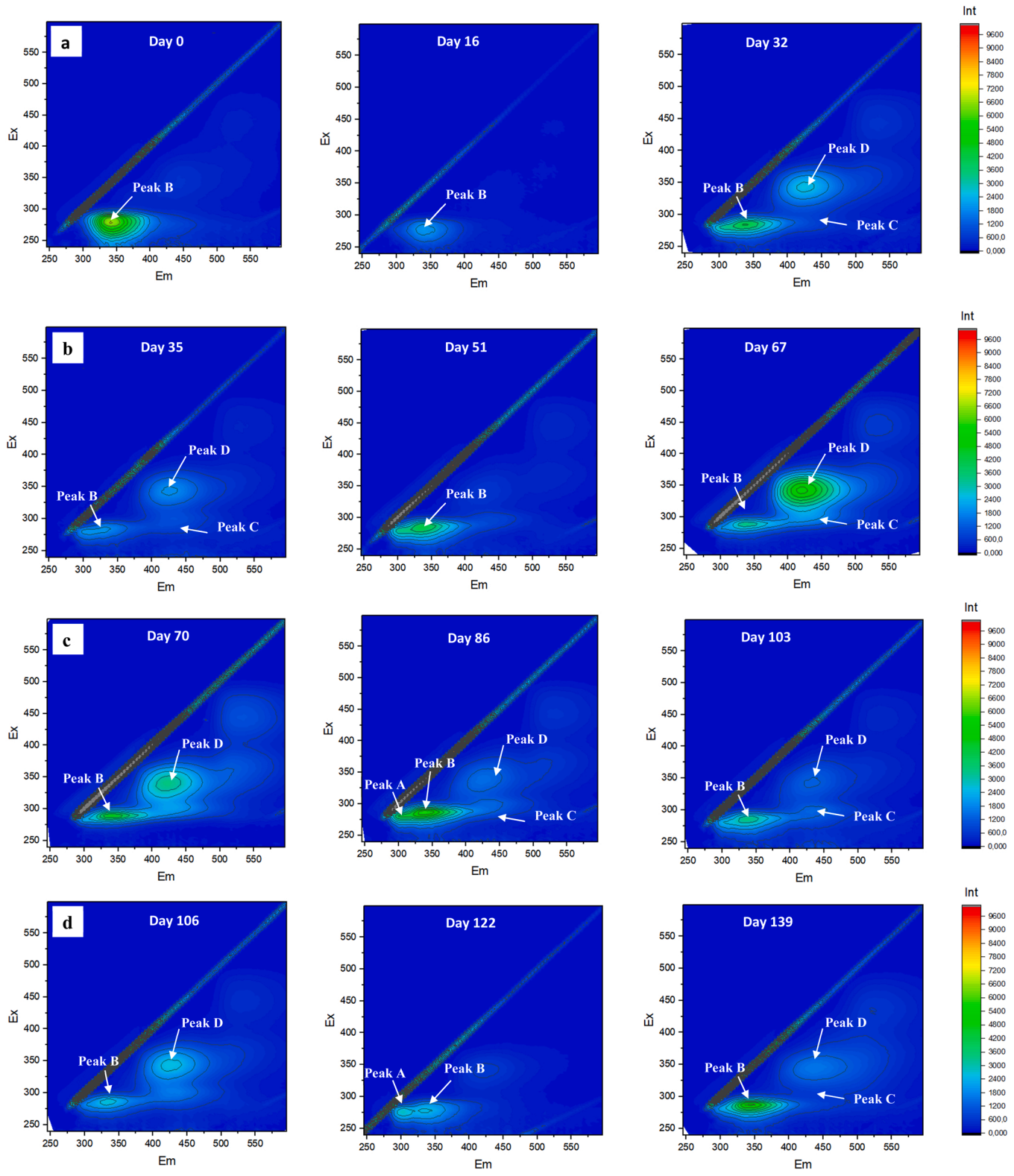

Fig. 3. 3D-EEM fluorescence spectra of LB-EPS under different DESL concentration: (a) phase I (0 mg L^{-1}); (b) phase II (1 mg L^{-1}); (c) phase III (5 mg L^{-1}); (d) phase IV (10 mg L^{-1}).

For TB-EPS, the chemical composition of EPS did not change significantly during phases I and II, mainly consisted of protein-like substances (peaks A and B) (Fig. 4a,b). Proteins-like substances displayed an increase in fluorescence intensity at the end of phase II (Fig. 4b), suggesting an increase in some functional groups, such as carboxyl, amino, hydroxyl and carbonyl [53]. After that, EPS composition increased humic and fulvic acid-like on day 86. The move of peak positions indicated chemical changes in the EPS components. The appearance and transformation of peak C and peak D during phase III (Fig. 4c), indicated chemical changes in the EPS components, probably by a complex formation between EPS and DESL. The study of Almutairi et al. [54] demonstrated that the fluorescence intensity of

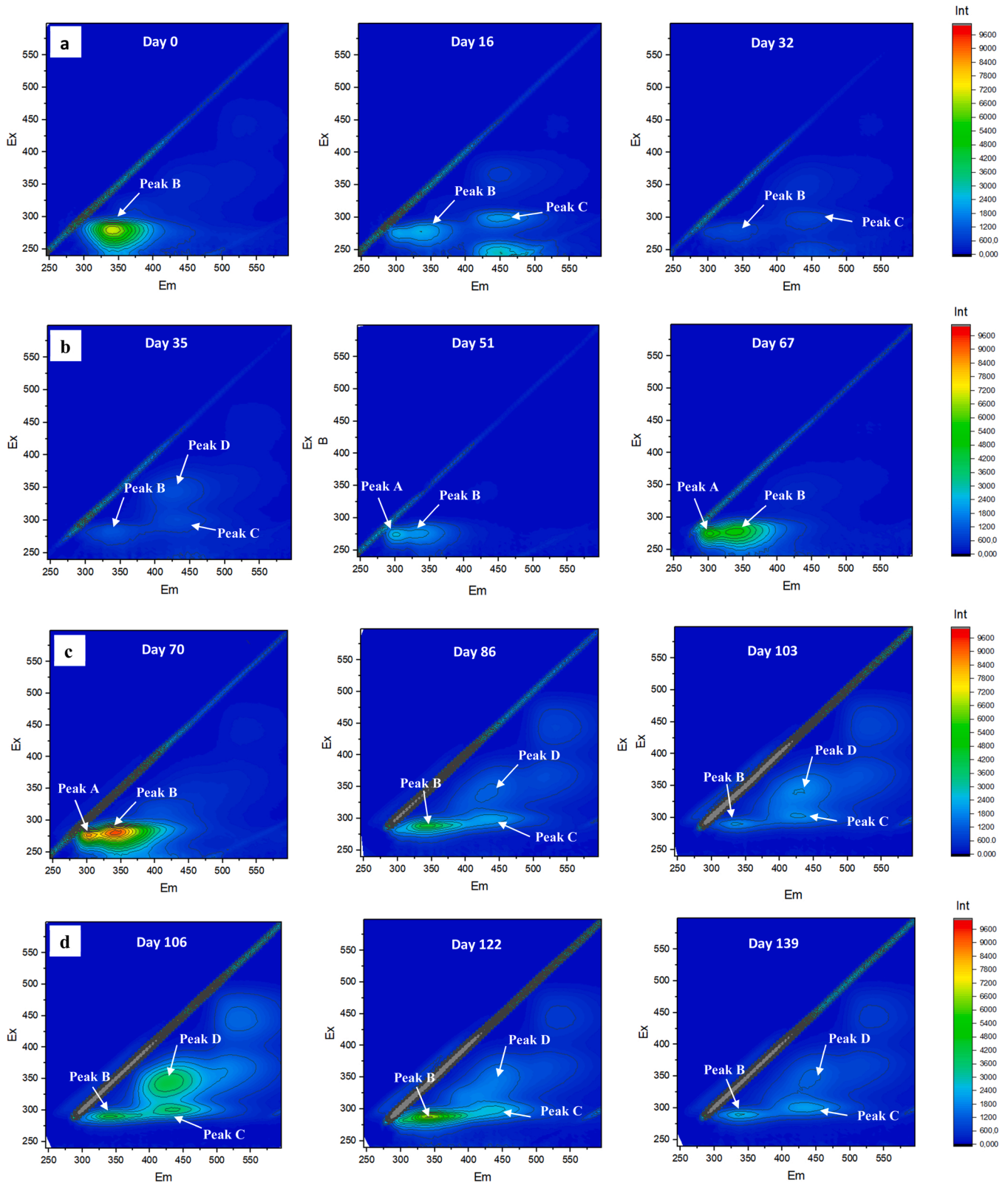

Fig. 4. 3D-EEM fluorescence spectra of TB-EPS under different DESL concentration: (a) phase I (0 mg L^{-1}); (b) phase II (1 mg L^{-1}); (c) phase III (5 mg L^{-1}); (d) phase IV (10 mg L^{-1}).

glycoproteins is quenched by loratadine (parent compound of DESL). The Gibb's free energy change was found to be negative for the interaction of loratadine with acid glycoprotein, indicating that the binding process is spontaneous. These authors also observed that hydrogen bonding and hydrophobic interactions were the main bonding forces between glycoproteins–loratadine. The additional peaks further confirmed that the presence of 10 mg L^{-1} of DESL could promote the secretion of EPS with different functional groups (proteins, humic acids

Table 2
Peak fluorescence intensity of samples at beginning, middle and end of each phase.

LB-EPS	Peak Intensity				TB-EPS	Peak Intensity			
Day	A	B	C	D	Day	A	B	C	D
0	–	6600	–	–	**0**	–	7000	–	–
16	–	2000	–	–	**16**	–	2400	2000	–
32	–	4200	700	2500	**32**	–	900	800	–
35	–	1900	1000	1800	**35**	–	1000	700	900
51	–	4100	–	–	**51**	2000	2000	–	–
67	–	3300	1500	5500	**67**	5600	5100	–	–
70	–	4700	1800	3300	**70**	8200	9200	–	–
86	3900	5800	1300	1400	**86**	–	4400	2100	1200
103	–	3400	1200	1200	**103**	–	1900	1800	1800
106	–	2700	–	2500	**106**	–	4400	3700	4200
122	2500	2500	–	600	**122**	–	6600	2400	1600
139	–	5400	800	1500	**139**	–	2400	2200	1200

and fulvic acids substances) by bacteria. During phase III and phase IV, a decrease in fluorescence intensity in the 3D-EEM spectra was obtained, which accounted for the reduction of some functional groups, such as aromatic ring and conjugated bond in chain structures [55]. These findings are consistent with previous work that gave similar shifts of fluorescence intensity and peak location, indicating chemical changes of the EPS components when biofilm was exposed to CuO nanoparticles [22]. All location shifts of the fluorescence peaks could provide spectral information on the chemical structural changes, indicating the functional group changes of EPS during DESL exposure [56,57].

It was further calculated (Table 3) that the percent fluorescence response of region A decreased, on average, from 73.1% to 56.5% for LB-EPS and from 56.4% to 40.7% for TB-EPS. For region B, the percent fluorescence response increased from 26.9% to 43.5% for LB-EPS and from 43.6% to 59.3% for TB-EPS, on average. It was evident that the percent fluorescence response of protein-like substances (region A) decreased in phases with DESL, implying that protein-like substances, instead humic acid-like substances, were quenched in the presence of DESL. Thus, our results propose that proteins-like substances played a specific role in removing DESL, probably by giving sites to DESL adsorption and forming a complex DESL-PN EPS and then decreasing the percent fluorescence response, which is in accordance with previous literature [54].

3.3. Structural characterization

Fig. 5a shows the aggregates area percentage along phases I-IV. During phase I, a normal aggregates structure was found, with a considerable presence of intermediate aggregates (%$Area_{int}$ of 81%, on average). A significant increase in large aggregates (%$Area_{larg}$ from 40% to 67%) occurred during phases III and IV, pointing to a global trend to form larger structures as visualized by microscopy (SI – Fig. S4 and S5). The increase in large aggregates, especially during phases III and IV, had a close relationship with TB-EPS production, suggesting that the increase in DESL concentration induced the production of more TB-EPS leading to larger aggregates. In fact, the EPS are involved in the structure of microbial aggregates and in interactions between cells as well. Treating the same wastewater, a full-scale system with predominantly pinpoint flocs (diameter < 50 μm) had more LB-EPS than a lab-scale system with predominantly large flocs (diameter > 340 μm) with more TB-EPS content [49].

Table 3
Average percentage of fluorescence response [$P_{i,n}$ (%)] of LB-EPS and TB-EPS under different DESL concentration for each phase.

LB-EPS	$P_{i,n}$ (%) Region A	$P_{i,n}$ (%) Region B	TB-EPS	$P_{i,n}$ (%) Region A	$P_{i,n}$ (%) Region B
Phase I	73.06	26.94	**Phase I**	56.44	43.56
Phase II	51.12	48.88	**Phase II**	66.91	33.09
Phase III	51.31	48.69	**Phase III**	53.44	46.56
Phase IV	56.52	43.48	**Phase IV**	40.71	59.29

The SVI and MLSS results along operation are shown in Fig. 5b and Fig. 5c shows the total filament length per volume (TL/Vol), and the total filaments length per MLSS (TL/MLSS). During phase I, the SVI values were < 150 mL g^{-1}, although close to the threshold limit (Fig. 5b). TL/MLSS was $< 10{,}000$ mm mg^{-1} and TL/Vol was < 10 mm μL^{-1} throughout the SBR operation (Fig. 5c). The present results corroborate previous studies where good settling ability was obtained for sludge with SVI, TL/Vol and TL/MLSS lower than 150 mL g^{-1}, 10 mm μL^{-1} and 10,000 mm mg^{-1}, respectively [23,58,59]. Regarding phase II, SVI results were > 150 mL g^{-1}, and the sludge demonstrated meagre settling ability. However, microscope inspection did not show any evidence that the low settling ability was due to filamentous bulking since the TL/MLSS and TL/Vol were less than the threshold limits (Fig. 5c). In fact, these results corroborate the findings of Jin et al. [60] and Melo et al. [23], revealing that the dysfunction on sludge settling ability can be governed by different sludge characteristics, such as EPS. Therefore, low settling ability may be associated with floccular sludge surrounded by large contents of LB-EPS during phase II (Fig. 2a, SI – Table S4), which likely retained water in the sludge flocs structure producing poorly settling and poorly compacting sludge. At the end of phase II, SVI decreased to values quite lower than the threshold limit, demonstrating the strong influence of chemical properties of AS aggregates surface in influencing the sludge settling ability. Thus, the difference in the concentration of EPS components (PS, PN, and HAS) might explain the settling ability along phase II. In fact, looking at data from the start of phase II until day 49 (SVI of 227 mL g^{-1}), a positive correlation between LB-EPS (chiefly PN and HAS) and SVI was found (SI – Table S7). In addition, during phase II, the LB-EPS concentration was quite close to the TB-EPS, which increased the LB/TB EPS ratio, suggesting that when LB-EPS and TB-EPS concentrations are similar, a dysfunction on the settling ability occurs. On the other hand, from the middle to the end of phase II, the SVI decreased to values lower than the threshold limit and presented a negative correlation with TB-EPS, mainly PN and HAS components. During phases III and IV, the biomass presented the best settling ability with values of SVI < 100 mL g^{-1}. Interestingly, the aggregates become larger (Fig. 5a), containing quite compact structures without free filamentous bacteria (SI – Fig. S4, S5). This behaviour was accompanied by a sharp increase of MLSS (from 3.0 to 4.8 g L^{-1}) at the beginning of phase IV. Also, our results imply that the fluctuation of MLSS during the experiment did not influence the biomass settling ability (Fig. 5b) since, for the same concentration of MLSS, different SVI results were found. This fact clearly demonstrates the contribution of aggregates structure to the settling ability quality. It can be reasonable to assume that other factors, such as chemical properties of AS aggregates, probably influenced by the change in the EPS composition and concentration, especially TB-EPS, had a key role to microbial aggregates become larger during phases III and IV.

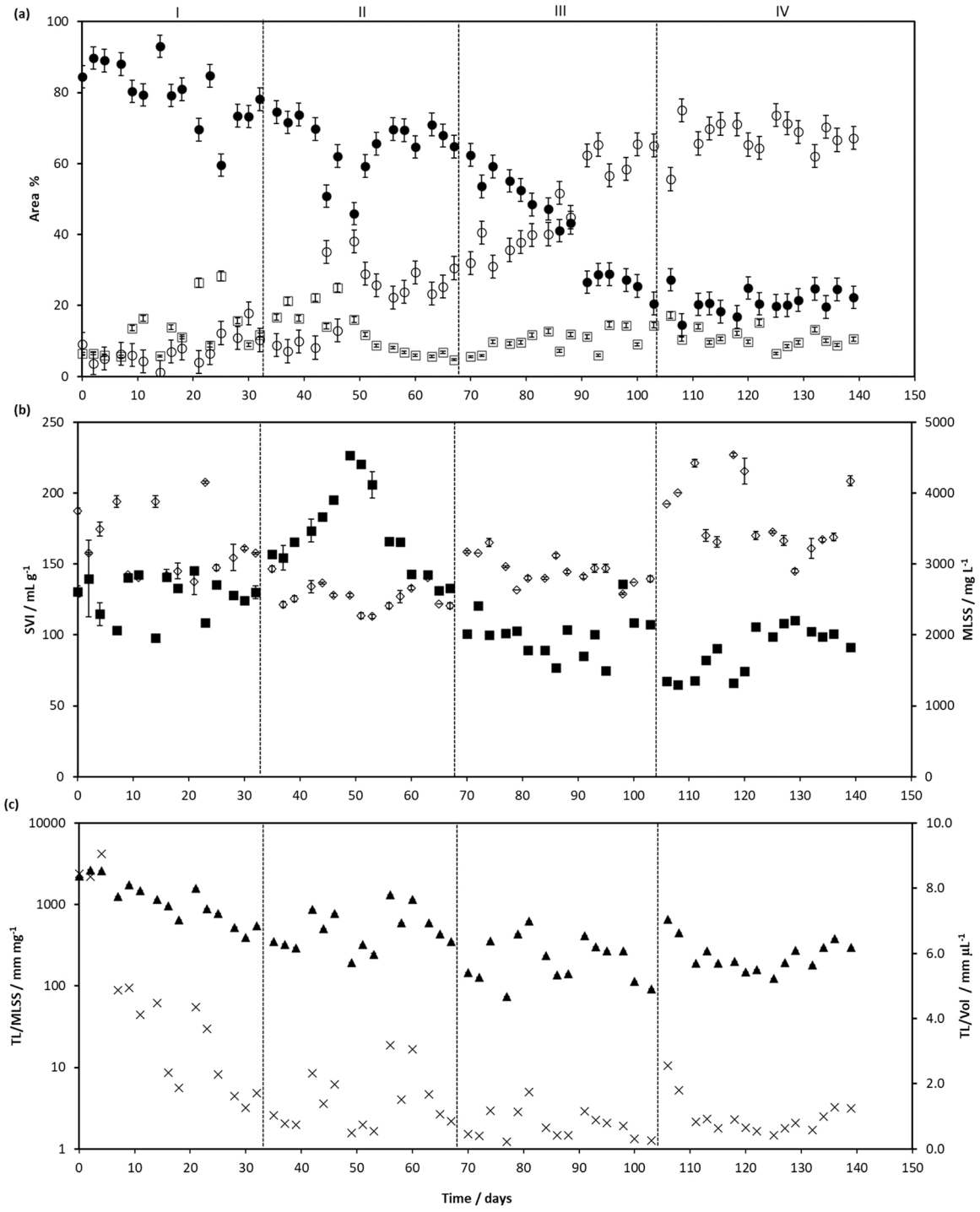

Fig. 5. (a) Area percentage for small (sml) (□), intermediate (int) (●), and large (larg) aggregates (○); (b) SVI (■) and MLSS (◊); (c) total filaments length per MLSS (TL/MLSS) (▲) and total filament length per volume (TL/Vol) (×). Operational phases I-IV.

These results agree with previous studies reporting the influence of EPS on aggregates size [47,49].

3.4. Principal component analysis

The PCA encompassed the QIA parameters (TL/MLSS, TL/Vol, equivalent diameter - Deq and %Area), biomass properties (MLVSS and SVI), and EPS and its components (Fig. 6a). PC1 and PC2 explained 36% and 21% of the original dataset variance, respectively, and were used in this analysis. Each operational phase was clearly identified in Fig. 6a. Phase I was characterized by presenting positive PC1 values and mainly negative PC2 values. On the other hand, positive values for PC2 could be inferred for phases II and III. Moreover, both operational periods differed in terms of PC1 values, being phase II on the positive side and phase III on the negative side. In addition, in the bottom left quadrant, phase IV was characterized by negative values for both PC1 and PC2.

With respect to the variable's importance in Fig. 7, it should be stressed that PC1 (Fig. 7a) was positively influenced by the $Area_{int}$, Deq_{sml}, filamentous bacteria content (TL/Vol and TL/MLSS), and SVI. Negative values for PC1 were severely influenced by the overall EPS content, mainly TB-EPS components, MLVSS and large aggregates characteristics (Deq_{larg} and $\%Area_{larg}$). On the other hand, PC2 (Fig. 7b)

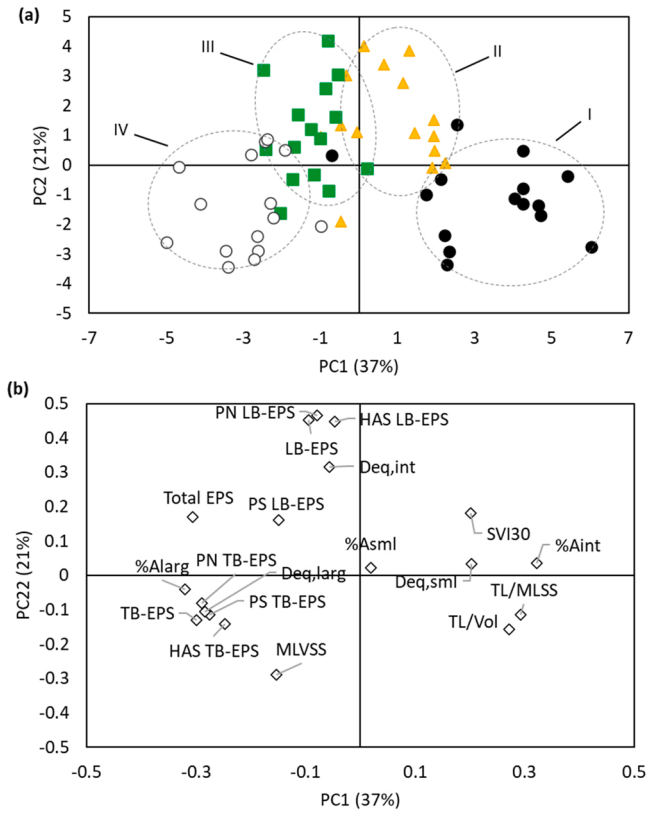

Fig. 6. PCA scores plot of the SBR operational parameters, EPS and QIA dataset for PC1 versus PC2. (a) phase I (●), phase II (▲), phase III (■), and phase IV (○); (b) Variables loadings plot of the PC1 and PC2.

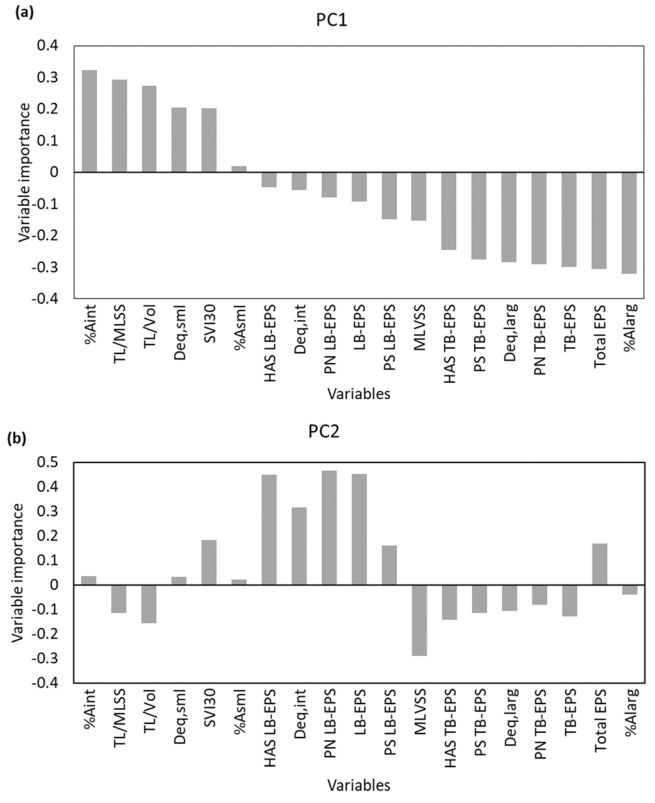

Fig. 7. Variable importance for PC1 and PC2, regarding the PCA of Fig. 6. (a) Variable importance for PC1; (b) Variable importance for PC2.

was positively influenced by the Total EPS, LB-EPS and its components, Deq_{int}, and SVI. Negative values for PC2 were influenced by the MLVSS, filamentous bacteria content (TL/MLSS, TL/Vol) and $\%Area_{larg}$, TB-EPS and its components.

Concerning the variable loadings presented in Fig. 6b, the SVI showed a close relationship with TL/MLSS and TL/Vol, Deq_{sml}, and $\%Area_{int}$. Furthermore, the results presented a strong relationship of AS aggregates (Deq_{larg} and $\%Area_{larg}$) with the EPS_{total} and TB-EPS and its components (PS, PN and HAS). Additionally, a close relationship was found between Deq_{int} and LB-EPS and its components (PN and HAS).

Differences observed in clusters (Fig. 6a) from PCA results are in accordance with the evolution of biomass behaviour. Phase I differed significantly from phases II, III and IV where the lowest values for overall EPS and the highest filamentous bacteria content were achieved. In addition, the difference between phase II and phase III could be explained by the increase of LB-EPS content (mainly HAS, PN and LB-EPS). In fact, these results could be explained by a somewhat similar biomass behaviour in terms of LB-EPS and its components during both operational periods (PC2) and different aggregate's structure (PC1), mainly $\%Area_{int}$ versus $\%Area_{larg}$ with an accentuated change in the middle of phase III. Phase IV was totally opposite from other phases, being influenced by TB-EPS content, lowest values of filamentous content (TL/Vol and TL/MLSS), and large aggregates structure (Deq_{larg}, $\%Area_{larg}$).

As previously observed, during phases II and III, high LB-EPS concentrations were obtained, especially PN and HAS components, which positively influenced the variation in PC2 suggesting chemical properties change in the surface of AS. EPS can differ in molecular weight and composition, mainly when produced under different conditions by microorganisms in biological systems [61]. Thus, these variations in LB-EPS can be related with the biomass response to DESL addition along phases II and III since LB-EPS content decreased again during phase IV (as shown in Fig. 2a).

Summarizing, our results suggest that TB-EPS and its components influence the structure of aggregates, which can be positively related to the large aggregates (Deq_{larg}, $\%Area_{larg}$) and negatively related to the small and intermediate aggregates (Deq_{sml}, $\%Area_{sml}$, $\%Area_{int}$). Hence, large aggregates formation can be associated with the high levels of EPS produced by biomass, supporting previous findings [47]. Beyond these results, aggregates were found with a large structure where cells were compactly packed during phases III and IV (SI – Figs. S4, S5). This might explain the good settling ability during these phases. In fact, these results are in accordance with previous studies that found EPS as key players in granules formation and stability [15,47,62]. Nevertheless, the LB-EPS and its components (PS, PN and HAS) correlated positively only with the Deq_{int}. Globally, we can infer that TB-EPS components have a more critical role in aggregates' structure than LB-EPS components.

4. Conclusions

COD and ammonium efficiency decreased, on average, from phase II to IV in the presence of DESL. Concerning the removal of DESL, just for the highest concentration (10 mg L^{-1}), the biomass significantly reduced its capacity compared to phases II and III. An increase in LB-EPS concentration during phases II and III with a subsequent reduction in phase IV, suggests that this variation could be a response of the biomass in SBR to DESL exposure. For TB-EPS, an increasing trend was observed, indicating a self-defence behaviour of the microorganisms in SBR towards DESL exposure. The 3D-EEM spectral analysis indicated that the primary components of LB-EPS and TB-EPS were protein-like substances, humic acid-like substances, and fulvic acid-like substances. Protein-like fluorophores were the key components in the sludge, which probably contributed to the formation and structural stability of large aggregates. QIA was valuable in understanding the changes in biomass properties over the experimental phases, demonstrating, for instance, that during phase II the low settling ability was unrelated to the

filamentous bacteria content. Finally, PCA results suggest that EPS, especially TB-EPS, significantly influenced aggregates structural parameters rather than LB-EPS.

CRediT authorship contribution statement

Antonio Melo: Investigation, Formal analysis, Writing – original draft. **Joana Costa**: Investigation, Software, Formal analysis. **Cristina Quintelas**: Investigation, Formal analysis, Writing – review & editing. **Eugénio C. Ferreira**: Supervision, Writing – review & editing, Funding raising. **Daniela P. Mesquita**: Conceptualization, Supervision, Writing - review & editing.

Declaration of Competing Interest

The authors declare that they have no known competing financial interests or personal relationships that could have appeared to influence the work reported in this paper.

Data Availability

Data will be made available on request.

Acknowledgments

The authors thank the Portuguese Foundation for Science and Technology (FCT) under the scope of the strategic funding of UIDB/04469/2020 unit, and by LABBELS – Associate Laboratory in Biotechnology, Bioengineering and Microelectromechanical Systems, LA/P/0029/2020. The authors also acknowledge the financial support to Antonio Melo through the grant number 240-20170220 provided by Instituto Federal de Educação, Ciência e Tecnologia de Pernambuco (IFPE). Daniela P. Mesquita and Cristina Quintelas thank FCT for funding through program DL 57/2016 – Norma transitória.

Appendix A. Supporting information

Supplementary data associated with this article can be found in the online version at doi:10.1016/j.jece.2022.108415.

References

[1] G.A. Loraine, M.E. Pettigrove, Seasonal variations in concentrations of pharmaceuticals and personal care products in drinking water and reclaimed wastewater in Southern California, Environ. Sci. Technol. 40 (2006) 687–695, https://doi.org/10.1021/es051380x.

[2] P. Chaturvedi, P. Shukla, B.S. Giri, P. Chowdhary, R. Chandra, P. Gupta, A. Pandey, Prevalence and hazardous impact of pharmaceutical and personal care products and antibiotics in environment: a review on emerging contaminants, Environ. Res. 194 (2021), 110664, https://doi.org/10.1016/j.envres.2020.110664.

[3] O. Golovko, V. Kumar, G. Fedorova, T. Randak, R. Grabic, Seasonal changes in antibiotics, antidepressants/psychiatric drugs, antihistamines and lipid regulators in a wastewater treatment plant, Chemosphere 111 (2014) 418–426, https://doi.org/10.1016/j.chemosphere.2014.03.132.

[4] L.A. Kristofco, B.W. Brooks, Global scanning of antihistamines in the environment: analysis of occurrence and hazards in aquatic systems, Sci. Total Environ. 592 (2017) 477–487, https://doi.org/10.1016/j.scitotenv.2017.03.120.

[5] F.E.R. Simons, K.J. Simons, Histamine and H1-antihistamines: celebrating a century of progress, J. Allergy Clin. Immunol. 128 (2011), https://doi.org/10.1016/j.jaci.2011.09.005.

[6] B. Kasprzyk-Hordern, R.M. Dinsdale, A.J. Guwy, The removal of pharmaceuticals, personal care products, endocrine disruptors and illicit drugs during wastewater treatment and its impact on the quality of receiving waters, Water Res 43 (2009) 363–380, https://doi.org/10.1016/j.watres.2008.10.047.

[7] J. Fick, H. Söderström, R.H. Lindberg, C. Phan, M. Tysklind, D.G.J. Larsson, Contamination of surface, ground, and drinking water from pharmaceutical production, Environ. Toxicol. Chem. 28 (2009) 2522, https://doi.org/10.1897/09-073.1.

[8] B. Du, S.P. Haddad, A. Luek, W.C. Scott, G.N. Saari, S.R. Burket, C.S. Breed, M. Kelly, L. Broach, J.B. Rasmussen, C.K. Chambliss, B.W. Brooks, Bioaccumulation of human pharmaceuticals in fish across habitats of a tidally influenced urban bayou, Environ. Toxicol. Chem. 35 (2016) 966–974, https://doi.org/10.1002/etc.3221.

[10] D.G.J. Larsson, C. de Pedro, N. Paxeus, Effluent from drug manufactures contains extremely high levels of pharmaceuticals, J. Hazard. Mater. 148 (2007) 751–755, https://doi.org/10.1016/j.jhazmat.2007.07.008.

[11] M.R. Iesce, M. Lavorgna, C. Russo, C. Piscitelli, M. Passananti, F. Temussi, M. DellaGreca, F. Cermola, M. Isidori, Ecotoxic effects of loratadine and its metabolic and light-induced derivatives, Ecotoxicol. Environ. Saf. 170 (2019) 664–672, https://doi.org/10.1016/j.ecoenv.2018.11.116.

[12] M.-Y. Chen, D.-J. Lee, J.-H. Tay, K.-Y. Show, Staining of extracellular polymeric substances and cells in bioaggregates, Appl. Microbiol. Biotechnol. 75 (2007) 467–474, https://doi.org/10.1007/s00253-006-0816-5.

[13] B.S. McSwain, R.L. Irvine, M. Hausner, P.A. Wilderer, Composition and distribution of extracellular polymeric substances in aerobic flocs and granular sludge, Appl. Environ. Microbiol. 71 (2005) 1051–1057, https://doi.org/10.1128/AEM.71.2.1051-1057.2005.

[14] B.M. Wilén, D. Lumley, A. Mattsson, T. Mino, Relationship between floc composition and flocculation and settling properties studied at a full scale activated sludge plant, Water Res. 42 (2008) 4404–4418, https://doi.org/10.1016/j.watres.2008.07.033.

[15] X. Hou, S. Liu, Z. Zhang, Role of extracellular polymeric substance in determining the high aggregation ability ofanammox sludge, Water Res 75 (2015) 51–62, https://doi.org/10.1016/j.watres.2015.02.031.

[16] A.C. Avella, L.F. Delgado, T. Görner, C. Albasi, M. Galmiche, P. de Donato, Effect of cytostatic drug presence on extracellular polymeric substances formation in municipal wastewater treated by membrane bioreactor, Bioresour. Technol. 101 (2010) 518–526, https://doi.org/10.1016/j.biortech.2009.08.057.

[17] G.-P. Sheng, H.-Q. Yu, X.-Y. Li, Extracellular polymeric substances (EPS) of microbial aggregates in biological wastewater treatment systems: a review, Biotechnol. Adv. 28 (2010) 882–894, https://doi.org/10.1016/j.biotechadv.2010.08.001.

[18] A.L. Amaral, M. Da Motta, M.N. Pons, H. Vivier, N. Roche, M. Mota, E.C. Ferreira, Survey of Protozoa and Metazoa populations in wastewater treatment plants by image analysis and discriminant analysis, Environmetrics 15 (2004) 381–390, https://doi.org/10.1002/env.652.

[19] D.P. Mesquita, A.L. Amaral, E.C. Ferreira, Identifying different types of bulking in an activated sludge system through quantitative image analysis, Chemosphere 85 (2011) 643–652, https://doi.org/10.1016/j.chemosphere.2011.07.012.

[20] C.S. Leal, M. Lopes, A. Val del Río, C. Quintelas, P.M.L. Castro, E.C. Ferreira, A. L. Amaral, D.P. Mesquita, Assessment of an aerobic granular sludge system in the presence of pharmaceutically active compounds by quantitative image analysis and chemometric techniques, J. Environ. Manag. 289 (2021), https://doi.org/10.1016/j.jenvman.2021.112474.

[21] L. Zhu, J. Zhou, M. Lv, H. Yu, H. Zhao, X. Xu, Specific component comparison of extracellular polymeric substances (EPS) in flocs and granular sludge using EEM and SDS-PAGE, Chemosphere 121 (2015) 26–32, https://doi.org/10.1016/j.chemosphere.2014.10.053.

[22] L. Miao, C. Wang, J. Hou, P. Wang, Y. Ao, Y. Li, Y. Yao, B. Lv, Y. Yang, G. You, Y. Xu, Q. Gu, Response of wastewater biofilm to CuO nanoparticle exposure in terms of extracellular polymeric substances and microbial community structure, Sci. Total Environ. 579 (2017) 588–597, https://doi.org/10.1016/j.scitotenv.2016.11.056.

[23] A. Melo, J. Costa, C. Quintelas, E.C. Ferreira, D.P. Mesquita, Effect of ibuprofen on extracellular polymeric substances (EPS) production and composition, and assessment of microbial structure by quantitative image analysis, J. Environ. Manag. 293 (2021), https://doi.org/10.1016/j.jenvman.2021.112852.

[24] APHA. Standard Methods for the Examination of Water and Wastewater, twentieth ed., American P, 1998.

[25] C. Quintelas, A. Melo, M. Costa, D.P. Mesquita, E.C. Ferreira, A.L. Amaral, Environmentally-friendly technology for rapid identification and quantification of emerging pollutants from wastewater using infrared spectroscopy, Environ. Toxicol. Pharmacol. 80 (2020), 103458, https://doi.org/10.1016/j.etap.2020.103458.

[26] X.Y. Li, S.F. Yang, Influence of loosely bound extracellular polymeric substances (EPS) on the flocculation, sedimentation and dewaterability of activated sludge, Water Res 41 (2007) 1022–1030, https://doi.org/10.1016/j.watres.2006.06.037.

[27] W. Chen, P. Westerhoff, J.A. Leenheer, K. Booksh, Fluorescence excitation-emission matrix regional integration to quantify spectra for dissolved organic matter, Environ. Sci. Technol. 37 (2003) 5701–5710, https://doi.org/10.1021/es034354c.

[28] J. Yang, X. Liu, D. Wang, Q. Xu, Q. Yang, G. Zeng, X. Li, Y. Liu, J. Gong, J. Ye, H. Li, Mechanisms of peroxymonosulfate pretreatment enhancing production of short-chain fatty acids from waste activated sludge, Water Res 148 (2019) 239–249, https://doi.org/10.1016/j.watres.2018.10.060.

[29] J. Qian, X. He, P. Wang, B. Xu, K. Li, B. Lu, W. Jin, S. Tang, Effects of polystyrene nanoplastics on extracellular polymeric substance composition of activated sludge: The role of surface functional groups, Environ. Pollut. 279 (2021), 116904, https://doi.org/10.1016/j.envpol.2021.116904.

[30] L. Pasquini, C. Merlin, L. Hassenboehler, J.F. Munoz, M.N. Pons, T. Görner, Impact of certain household micropollutants on bacterial behavior. Toxicity tests/study of extracellular polymeric substances in sludge, Sci. Total Environ. 463–464 (2013) 355–365, https://doi.org/10.1016/j.scitotenv.2013.06.018.

[31] Y. Jia, L. Yin, S.K. Khanal, H. Zhang, A.S. Oberoi, H. Lu, Biotransformation of ibuprofen in biological sludge systems: Investigation of performance and mechanisms, Water Res 170 (2020), 115303, https://doi.org/10.1016/j.watres.2019.115303.

[32] J. Peng, X. Wang, F. Yin, G. Xu, Characterizing the removal routes of seven pharmaceuticals in the activated sludge process, Sci. Total Environ. 650 (2019) 2437–2445, https://doi.org/10.1016/j.scitotenv.2018.10.004.
[33] N. Henning, P. Falås, S. Castronovo, K.S. Jewell, K. Bester, T.A. Ternes, A. Wick, Biological transformation of fexofenadine and sitagliptin by carrier-attached biomass and suspended sludge from a hybrid moving bed biofilm reactor, Water Res 167 (2019), 115034, https://doi.org/10.1016/j.watres.2019.115034.
[34] S.J. Khan, J.E. Ongerth, Modelling of pharmaceutical residues in Australian sewage by quantities of use and fugacity calculations, Chemosphere 54 (2004) 355–367, https://doi.org/10.1016/j.chemosphere.2003.07.001.
[35] M. Boehler, B. Zwickenpflug, J. Hollender, T. Ternes, A. Joss, H. Siegrist, Removal of micropollutants in municipal wastewater treatment plants by powder-activated carbon, Water Sci. Technol. 66 (2012) 2115–2121, https://doi.org/10.2166/wst.2012.353.
[36] J. Kosonen, L. Kronberg, The occurrence of antihistamines in sewage waters and in recipient rivers, Environ. Sci. Pollut. Res. 16 (2009) 555–564, https://doi.org/10.1007/s11356-009-0144-2.
[37] J. Li, X. Liu, Y. Liu, J. Ramsay, C. Yao, R. Dai, The effect of continuous exposure of copper on the properties and extracellular polymeric substances (EPS) of bulking activated sludge, Environ. Sci. Pollut. Res. 18 (2011) 1567–1573, https://doi.org/10.1007/s11356-011-0492-6.
[38] C. Li, C. Cabassud, B. Reboul, C. Guigui, Effects of pharmaceutical micropollutants on the membrane fouling of a submerged MBR treating municipal wastewater: Case of continuous pollution by carbamazepine, Water Res 69 (2015) 183–194, https://doi.org/10.1016/j.watres.2014.11.027.
[39] J. Ma, X. Quan, X. Si, Y. Wu, Responses of anaerobic granule and flocculent sludge to ceria nanoparticles and toxic mechanisms, Bioresour. Technol. 149 (2013) 346–352, https://doi.org/10.1016/j.biortech.2013.09.080.
[40] C. Song, X.F. Sun, S.F. Xing, P.F. Xia, Y.J. Shi, S.G. Wang, Characterization of the interactions between tetracycline antibiotics and microbial extracellular polymeric substances with spectroscopic approaches, Environ. Sci. Pollut. Res. 21 (2014) 1786–1795, https://doi.org/10.1007/s11356-013-2070-6.
[41] Q. Kong, X. He, Y. Feng, M. sheng Miao, Q. Wang, Y. da Du, F. Xu, Pollutant removal and microorganism evolution of activated sludge under ofloxacin selection pressure, Bioresour. Technol. 241 (2017) 849–856, https://doi.org/10.1016/j.biortech.2017.06.019.
[42] G. Zhou, N. Li, E.R. Rene, Q. Liu, M. Dai, Q. Kong, Chemical composition of extracellular polymeric substances and evolution of microbial community in activated sludge exposed to ibuprofen, J. Environ. Manag. 246 (2019) 267–274, https://doi.org/10.1016/j.jenvman.2019.05.044.
[43] W. An, F. Guo, Y. Song, N. Gao, S. Bai, J. Dai, H. Wei, L. Zhang, D. Yu, M. Xia, Y. Yu, M. Qi, C. Tian, H. Chen, Z. Wu, T. Zhang, D. Qiu, Comparative genomics analyses on EPS biosynthesis genes required for floc formation of Zoogloea resiniphila and other activated sludge bacteria, Water Res. 102 (2016) 494–504, https://doi.org/10.1016/j.watres.2016.06.058.
[44] H. Zhang, S. Song, Y. Jia, D. Wu, H. Lu, Stress-responses of activated sludge and anaerobic sulfate-reducing bacteria sludge under long-term ciprofloxacin exposure, Water Res. 164 (2019), https://doi.org/10.1016/j.watres.2019.114964.
[45] X. Tian, Z. Shen, Z. Han, Y. Zhou, The effect of extracellular polymeric substances on exogenous highly toxic compounds in biological wastewater treatment: An overview, Bioresour. Technol. Rep. 5 (2019) 28–42, https://doi.org/10.1016/j.biteb.2018.11.009.
[46] Y. Li, M. Xin, D. Xie, S. Fan, J. Ma, K. Liu, F. Yu, Variation in extracellular polymeric substances from enterobacter sp. and their Pb2+adsorption behaviors, ACS Omega 6 (2021) 9617–9628, https://doi.org/10.1021/acsomega.1c00185.
[47] D. Xu, J. Liu, T. Ma, Y. Gao, S. Zhang, J. Li, Rapid granulation of aerobic sludge in a continuous-flow reactor with a two-zone sedimentation tank by the addition of dewatered sludge, J. Water Process Eng. 41 (2021), 101941, https://doi.org/10.1016/j.jwpe.2021.101941.
[48] P.H. Santschi, W.C. Chin, A. Quigg, C. Xu, M. Kamalanathan, P. Lin, R.F. Shiu, Marine gel interactions with hydrophilic and hydrophobic pollutants, Gels 7 (2021) 1–14, https://doi.org/10.3390/gels7030083.
[49] M. Basuvaraj, J. Fein, S.N. Liss, Protein and polysaccharide content of tightly and loosely bound extracellular polymeric substances and the development of a granular activated sludge floc, Water Res. 82 (2015) 104–117, https://doi.org/10.1016/j.watres.2015.05.014.
[50] G.P. Sheng, H.Q. Yu, Characterization of extracellular polymeric substances of aerobic and anaerobic sludge using three-dimensional excitation and emission matrix fluorescence spectroscopy, Water Res. 40 (2006) 1233–1239, https://doi.org/10.1016/j.watres.2006.01.023.
[51] L. Guo, M. Lu, Q. Li, J. Zhang, Y. Zong, Z. She, Three-dimensional fluorescence excitation-emission matrix (EEM) spectroscopy with regional integration analysis for assessing waste sludge hydrolysis treated with multi-enzyme and thermophilic bacteria, Bioresour. Technol. 171 (2014) 22–28, https://doi.org/10.1016/j.biortech.2014.08.025.
[52] Z. Wang, M. Gao, Z. Wang, Z. She, Q. Chang, C. Sun, J. Zhang, Y. Ren, N. Yang, Effect of salinity on extracellular polymeric substances of activated sludge from an anoxic-aerobic sequencing batch reactor, Chemosphere 93 (2013) 2789–2795, https://doi.org/10.1016/j.chemosphere.2013.09.038.
[53] J. Chen, B. Gu, E.J. LeBoeuf, H. Pan, S. Dai, Spectroscopic characterization of the structural and functional properties of natural organic matter fractions, Chemosphere 48 (2002) 59–68, https://doi.org/10.1016/S0045-6535(02)00041-3.
[54] F.M. Almutairi, M.R. Ajmal, M.K. Siddiqi, A.I. Alalawy, R.H. Khan, On the binding reaction of loratadine with human serum acute phase protein alpha 1-acid glycoprotein, J. Biomol. Struct. Dyn. 0 (2021) 1–8, https://doi.org/10.1080/07391102.2021.1930164.
[55] J. Świetlik, A. Dąbrowska, U. Raczyk-Stanisławiak, J. Nawrocki, Reactivity of natural organic matter fractions with chlorine dioxide and ozone, Water Res. 38 (2004) 547–558, https://doi.org/10.1016/j.watres.2003.10.034.
[56] T. Liu, Z. lin Chen, W. zheng Yu, S. jie You, Characterization of organic membrane foulants in a submerged membrane bioreactor with pre-ozonation using three-dimensional excitation-emission matrix fluorescence spectroscopy, Water Res. 45 (2011) 2111–2121, https://doi.org/10.1016/j.watres.2010.12.023.
[57] L. Zhu, H. ying Qi, M. Le Lv, Y. Kong, Y.W. Yu, X.Y. Xu, Component analysis of extracellular polymeric substances (EPS) during aerobic sludge granulation using FTIR and 3D-EEM technologies, Bioresour. Technol. 124 (2012) 455–459, https://doi.org/10.1016/j.biortech.2012.08.059.
[58] J. Yao, J. Liu, Y. Zhang, S. Xu, Y. Hong, Y. Chen, Adding an anaerobic step can rapidly inhibit sludge bulking in SBR reactor, Sci. Rep. 9 (2019) 1–10, https://doi.org/10.1038/s41598-019-47304-3.
[59] A.L. Amaral, E.C. Ferreira, Activated sludge monitoring of a wastewater treatment plant using image analysis and partial least squares regression, Anal. Chim. Acta 544 (2005) 246–253, https://doi.org/10.1016/j.aca.2004.12.061.
[60] B. Jin, B.M. Wilén, P. Lant, A comprehensive insight into floc characteristics and their impact on compressibility and settleability of activated sludge, Chem. Eng. J. 95 (2003) 221–234, https://doi.org/10.1016/S1385-8947(03)00108-6.
[61] B.Q. Liao, H.J. Lin, S.P. Langevin, W.J. Gao, G.G. Leppard, Effects of temperature and dissolved oxygen on sludge properties and their role in bioflocculation and settling, Water Res. 45 (2011) 509–520, https://doi.org/10.1016/j.watres.2010.09.010.
[62] S.S. Adav, D.-J. Lee, J.-H. Tay, Extracellular polymeric substances and structural stability of aerobic granule, Water Res. 42 (2008) 1644–1650, https://doi.org/10.1016/j.watres.2007.10.013.